

Statistical mechanics of the N -queens problem

Zong-Yue Liu,¹ Hai-Jun Liao,² and Lei Wang²

¹*Kuang Yaming Honors School, Nanjing University, Nanjing 210093, China*

²*Institute of Physics, Chinese Academy of Sciences, Beijing 100190, China*

(Dated: May 11, 2026)

We investigate the N -queens problem as a lattice gas—a model in which N queens are placed on an $N \times N$ chessboard with pairwise repulsive interactions along shared rows, columns, and diagonals—from the perspective of statistical mechanics. The ground states are exactly the $Q(N)$ solutions of the classical N -queens problem, with entropy per queen $s_0 \approx \ln N - \gamma$ ($\gamma \approx 1.944$). This entropy reflects a characteristic constraint hierarchy: each successive geometric constraint—columns, then diagonals—reduces the entropy from the free-placement value $\ln N$ by a definite constant. We derive the exact high-temperature energy $E/N \rightarrow 5/3$ as $N \rightarrow \infty$. Extensive Monte Carlo simulations with 10^8 sweeps per temperature point for $N = 8$ – 1024 reveal that the specific heat per queen C_v/N converges to a universal function of T as $N \rightarrow \infty$. The converged curve features a non-divergent peak $C_v^{\max}/N \approx 1.63$ at $T^* \approx 0.235 J$, establishing the absence of a thermodynamic phase transition. Combined with the trivially exact high-temperature entropy $S(\infty)/N = \frac{1}{N} \ln \binom{N^2}{N}$, the convergence of C_v/N enables a thermodynamic integration of C_v/T from $T = \infty$ to $T = 0$ that recovers the ground-state entropy—and hence the Simkin constant γ —purely from Monte Carlo data. This provides an independent *thermodynamic* route to a fundamental combinatorial constant. Thermodynamic integration yields $\gamma_{\text{MC}} = 1.946 \pm 0.003$ at $N = 1024$, within 0.1% of the precise combinatorial value $\gamma = 1.94400(1)$. We further present a transfer-matrix-based tensor network formulation that encodes the non-attacking constraints into a rank-9 site tensor with 17 nonzero elements, providing a complementary exact-enumeration route.

I. INTRODUCTION

The N -queens problem—placing N mutually non-attacking queens on an $N \times N$ chessboard—is among the oldest combinatorial problems in mathematics, dating back to the work of Bezzel in 1848 [1]. Despite its long history, the asymptotic enumeration of solutions was resolved only recently. Simkin [2] proved that the number of solutions $Q(N)$ satisfies $Q(N) \sim (N/e^\gamma)^N$. This result builds on the breakthrough of Bowtell and Keevash [3] and earlier bounds by Luria and Simkin [4]. Simkin’s proof introduces *queenons*—limit objects defined as probability measures on the unit square—and characterizes γ as the solution of a convex optimization problem over this space; the upper bound employs the entropy method while the lower bound is established by a randomized construction algorithm, yielding $\gamma \in [1.939, 1.945]$. Nobel et al [5] subsequently refined these bounds to $\gamma = 1.94400(1)$ by solving Simkin’s convex programs with large-scale Newton methods. On the computational side, exact enumeration of $Q(N)$ by exhaustive backtracking search has been pushed to $N = 27$ using massively parallel GPU computation [6], highlighting the combinatorial explosion that limits direct counting to moderate board sizes. All of these determinations are purely combinatorial. In this work, we pursue an independent, thermodynamic route. The starting point is the entropy per queen implied by the asymptotic formula $Q(N) \sim (N/e^\gamma)^N$: $s_0 = \lim_{N \rightarrow \infty} \ln Q(N)/N = \ln N - \gamma$.

The form of this entropy is suggestive. On an $N \times N$ board with one queen per row—the row constraint being enforced by construction—each queen can occupy any of the N columns, giving $\ln N$ units of entropy per queen.

The N -queens entropy $s_0 = \ln N - \gamma$ can therefore be read as: each queen retains the full lattice entropy $\ln N$, reduced by a constant γ that encodes the cumulative cost of geometric constraints. This constant γ decomposes through a hierarchy of increasingly stringent geometric constraints [7]—column non-repetition costs one unit of entropy (the Stirling correction), and the two diagonal constraints cost a further $\gamma - 1 \approx 0.94$ units (see Sec. III A for details). That each constraint reduces the per-queen entropy by a well-defined constant, independent of N in the large- N limit, hints at a deeper statistical-mechanical structure underlying the combinatorics.

This additive decomposition of entropy into constraint costs motivates a statistical-mechanical approach. We map the N -queens problem to a lattice gas with tunable temperature [8, 9] and perform extensive Monte Carlo simulations. Throughout this paper we set $k_B = 1$, so that entropy is dimensionless and temperature has units of energy. A central finding is that the specific heat per queen, C_v/N , converges to a size-independent curve for sufficiently large N , exhibiting a Schottky-type peak but no phase transition. Combined with the exactly known high-temperature entropy $S(\infty)/N = \frac{1}{N} \ln \binom{N^2}{N} \approx \ln N + 1$, this convergence enables a thermodynamic integration

$$s_0 = \frac{S(\infty)}{N} - \int_0^\infty \frac{C_v}{NT} dT,$$

which extracts the ground-state entropy—and hence the Simkin constant γ —purely from Monte Carlo simulation data. This provides an independent *thermodynamic* route to γ : the only combinatorial input is the trivially exact high-temperature entropy $S(\infty)/N = \frac{1}{N} \ln \binom{N^2}{N}$,

while the Simkin–Nobel value is used solely for post-hoc comparison. Our thermodynamic extraction yields $\gamma_{\text{MC}} = 1.946 \pm 0.003$ at $N = 1024$ (within 0.1% of the precise value [5]); the monotonic convergence of γ_{MC} toward the asymptotic value with increasing N is shown in Fig. 4(b).

We also present a complementary exact counting approach based on tensor network contractions. Each non-attacking constraint—row, column, or diagonal—is encoded as a matrix product operator with bond dimension $D = 2$. Their intersection at every lattice site produces a rank-9 local tensor with only 17 nonzero elements. Exact contraction of the resulting network yields $Q(N)$ without statistical noise, providing independent benchmarks at moderate N .

The paper is organized as follows. Section II defines the model. Section III presents analytical results: the ground-state entropy and constraint hierarchy, and the exact high-temperature limit. Section IV presents Monte Carlo results. Section V carries out the thermodynamic integration. Section VI presents a tensor network formulation that provides an alternative exact-enumeration route. Section VII concludes with a discussion of the limitations of the Monte Carlo and tensor network approaches and open problems.

II. MODEL AND SIMULATION METHODOLOGY

We consider an $N \times N$ square lattice with open boundary conditions. Each site (i, j) ($i, j = 1, \dots, N$) carries an occupation variable $n_{ij} \in \{0, 1\}$. The Hamiltonian counts mutually attacking queen pairs:

$$H = J \sum_{\langle (i,j), (i',j') \rangle_{\text{attack}}} n_{ij} n_{i'j'}, \quad (1)$$

where the sum runs over all pairs sharing a row ($i = i'$), column ($j = j'$), main diagonal ($i - j = i' - j'$), or anti-diagonal ($i + j = i' + j'$), and $J > 0$. We set $J = 1$ throughout.

The lattice decomposes naturally into *attack lines*: N rows, N columns, $2N - 1$ main diagonals, and $2N - 1$ anti-diagonals. Writing n_α for the number of queens on line α , the Hamiltonian takes the compact form

$$H = \sum_{\alpha \in \mathcal{L}} \binom{n_\alpha}{2}, \quad (2)$$

where \mathcal{L} denotes the set of all $6N - 2$ attack lines and $\binom{n}{2} = n(n-1)/2$ counts the number of attacking pairs on each line. This decomposition into line contributions is the starting point for the high-temperature calculation (Sec. III B).

We work in the canonical ensemble with fixed particle number N —the natural choice since each valid N -queens configuration places exactly N queens—and use

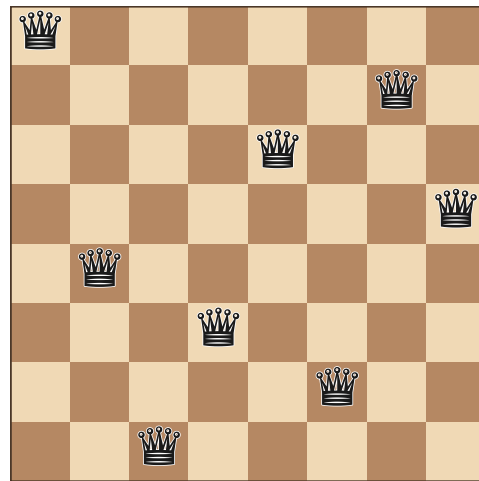


FIG. 1. One of the $Q(8) = 92$ non-attacking ground-state configurations on an 8×8 chessboard. No two queens share a row, column, or diagonal.

Kawasaki dynamics [10] (queen–vacancy exchange) with the Metropolis acceptance criterion [11]. We choose queen–vacancy rather than queen–queen exchanges because the former moves a single queen to any empty site on the board, allowing large spatial displacements in one step, whereas queen–queen swaps merely permute occupied sites and cannot efficiently explore configurations with different spatial structure. One *sweep* consists of N attempted exchanges. Statistical errors are estimated by jackknife resampling with 200 bins [12]. We simulate eight system sizes $N = 8, 16, 32, 64, 128, 256, 512, 1024$ on a uniform grid of 280 temperature points spanning $T = 0.05$ to $500 J$, with 10^8 measurement sweeps and 2×10^6 thermalization sweeps at every temperature point. The grid places 160 points in the specific-heat peak region ($T = 0.1025$ – $0.500 J$ in steps of $0.0025 J$), 11 points in the low-temperature region ($T = 0.050$ – $0.100 J$, step $0.005 J$), and the remaining 109 points at intermediate and high temperatures up to $T = 500 J$. All eight sizes use the same temperature grid and measurement parameters, ensuring a self-consistent data set. The simulations were carried out using 280 CPU cores in parallel, with each core handling all eight system sizes at a single temperature point in serial; the total wall-clock time was approximately nine hours. We verified ergodicity by running independent simulations from multiple random initial configurations (seeds); all runs yielded statistically consistent results for E/N and C_v/N at every temperature, confirming that the Kawasaki dynamics explores the configuration space adequately within our thermalization and measurement windows. A representative ground-state configuration is shown in Fig. 1.

TABLE I. Entropy per queen under successive constraints for the N -queens problem. The column constraint costs exactly 1 unit; the two diagonal constraints cost $\gamma - 1 \approx 0.94$ units combined.

Model	Constraints	Ω	$s = \frac{1}{N} \ln \Omega$
Free	Row only	N^N	$\ln N$
Permutation	Row + column	$N!$	$\ln N - 1$
N -queens	Row + col + 2 diag	$\approx (N/e^\gamma)^N$	$\ln N - \gamma$

III. ANALYTICAL RESULTS

A. Ground-state entropy and constraint hierarchy

For N queens, the ground states ($E = 0$) correspond to the $Q(N)$ non-attacking configurations. Since $Q(N) \sim (N/e^\gamma)^N$, the entropy per queen is

$$s_0 = \lim_{N \rightarrow \infty} \frac{\ln Q(N)}{N} = \ln N - \gamma, \quad \gamma = 1.94400(1). \quad (3)$$

The three-level constraint hierarchy (Table I), implicit in the Stirling approximation and Simkin's result [2, 7], provides a useful physical interpretation. Starting from a fully unconstrained model where each queen independently chooses one of N columns ($\Omega_{\text{free}} = N^N$, $s_{\text{free}} = \ln N$), the column non-repetition constraint reduces the count to $N!$ permutations. By Stirling's approximation, $\ln N! = N \ln N - N + O(\ln N)$, so the entropy per queen is

$$s_{\text{perm}} = \frac{\ln N!}{N} = \ln N - 1 + O\left(\frac{\ln N}{N}\right). \quad (4)$$

Thus the column constraint costs exactly one unit of entropy—the Stirling correction arising from the non-repetition constraint on column assignments.

The two diagonal constraints further reduce the entropy to $s_0 = \ln N - \gamma$, costing an additional $\gamma - 1 \approx 0.94$ units, or approximately $(\gamma - 1)/2 \approx 0.47$ units per diagonal family. The hierarchy of costs is physically natural: the column constraint, being a global permutation on N equivalent lines, removes exactly one unit of freedom per queen, while each diagonal family—whose lines have unequal lengths ranging from 1 to N —removes roughly half a unit.

That each geometric constraint reduces the per-queen entropy by a constant independent of N suggests that the finite-temperature thermodynamics may also admit a simple analytical description. We turn to this question next, beginning with the high-temperature limit.

B. High-temperature limit

At $T \rightarrow \infty$, all $\binom{N^2}{N}$ configurations are equally probable. Following Polson and Sokolov [9], the exact per-queen energy can be obtained by linearity of expectation

over the attack-line decomposition [Eq. (2)]. The probability that any two given sites are simultaneously occupied is $P = N(N-1)/[N^2(N^2-1)]$, and the total number of attacking site pairs summed over all $6N-2$ lines is $S_{\text{tot}} = N(N-1)(5N-1)/3$. Combining these gives the exact result

$$\left. \frac{\langle E \rangle}{N} \right|_{T \rightarrow \infty} = \frac{(5N-1)(N-1)}{3N(N+1)} \xrightarrow{N \rightarrow \infty} \frac{5}{3}, \quad (5)$$

valid for all finite N . Our Monte Carlo simulations (Fig. 3) confirm this: at high T , E/N converges to Eq. (5) with corrections of order $O(1/N)$.

IV. FINITE-TEMPERATURE MONTE CARLO RESULTS

A. Convergence diagnostics

Before presenting thermodynamic observables, we verify that the Monte Carlo simulations have reached equilibrium and that the measurements are statistically independent. Figure 2 shows the acceptance rate and the integrated autocorrelation time τ_{int} of the energy as functions of temperature for several system sizes.

The acceptance rate [panel (a)] increases monotonically with T , reaching ~ 0.38 – 0.47 at $T = 1 J$; it drops below 10^{-5} for $T \lesssim 0.1 J$, reflecting the near-perfect freezing into non-attacking ground states. For $N \geq 32$ the curves collapse, confirming convergence to the thermodynamic limit.

The autocorrelation time [panel (b)] exhibits a sharp peak at $T \approx 0.055$ – $0.10 J$, well below the specific heat maximum $T^* \approx 0.235 J$, reaching $\tau_{\text{int}} \approx 5.0 \times 10^4$ sweeps for $N = 1024$. Even at this worst case, 10^8 measurement sweeps yield ~ 2000 independent samples—adequate for the essentially featureless low-temperature regime where both E/N and C_v/N approach zero exponentially. Crucially, at the physically important specific heat peak ($T \approx 0.235 J$), $\tau_{\text{int}} \approx 85$ – 200 sweeps for all N , providing more than 5×10^5 independent samples per temperature point and ensuring high statistical precision in the region that matters most. At $T/J > 0.4$, τ_{int} falls to ~ 5 – 10 sweeps for all system sizes. We additionally verified ergodicity by comparing independent runs from different random initial configurations, all yielding statistically consistent results.

B. Energy

Figure 3 shows E/N vs. T for $N = 8$ – 1024 . The curves for $N \geq 32$ are nearly indistinguishable, confirming rapid convergence to the thermodynamic limit. At high temperatures, E/N approaches the exact finite- N value [Eq. (5)], which itself converges to $5/3$ as $N \rightarrow \infty$.

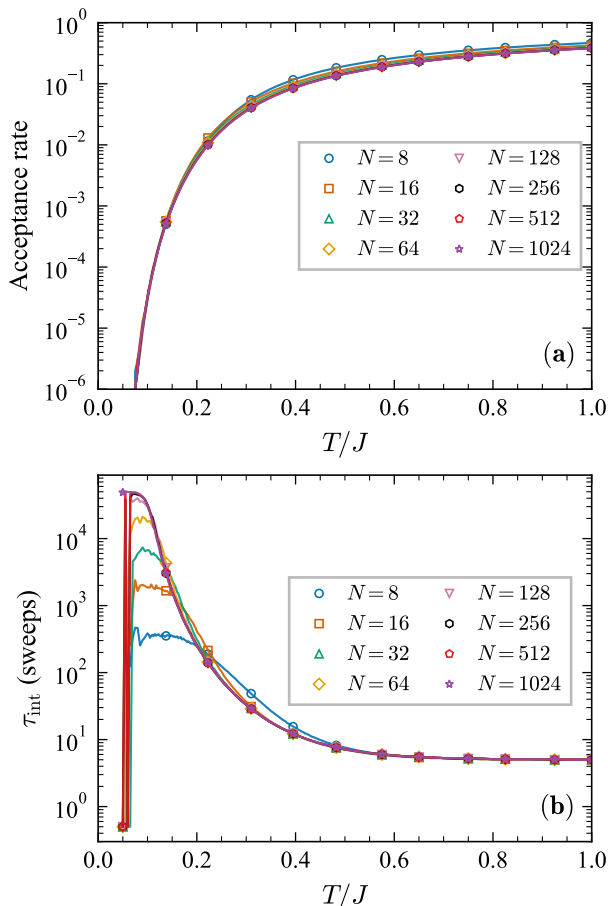


FIG. 2. Convergence diagnostics for the Monte Carlo simulations. (a) Acceptance rate of the Kawasaki (queen–vacancy exchange) moves as a function of temperature for $N = 8$ –1024 (log scale). The rate drops below 10^{-5} for $T \lesssim 0.1 J$ and rises monotonically, reaching 0.38–0.47 at $T = 1 J$. (b) Integrated autocorrelation time τ_{int} of the energy in units of sweeps (log scale). The sharp peak at $T \approx 0.055$ – $0.10 J$ reflects low-temperature freezing and lies well below the specific heat maximum $T^* \approx 0.235 J$; at T^* itself, $\tau_{\text{int}} \approx 85$ – 200 sweeps, yielding more than 5×10^5 independent samples from 10^8 sweeps.

C. Specific heat convergence

The specific heat per queen $C_v/N = (\langle E^2 \rangle - \langle E \rangle^2)/(T^2 N)$ is shown in Fig. 4(a). For $N \geq 32$, the C_v/N curves collapse onto a single function of T , indicating that the thermodynamic limit has been reached. Table II lists the peak values.

The key observation is that C_v^{max}/N saturates near 1.63 for $N \geq 32$ and shows no systematic growth with system size (Table II). The variation across $N = 32$ – 1024 is $\Delta C_v^{\text{max}}/N \lesssim 0.007$, far smaller than the ~ 0.06 per doubling expected from a logarithmic divergence $\propto \ln N$. This behavior is consistent with the absence of a thermo-

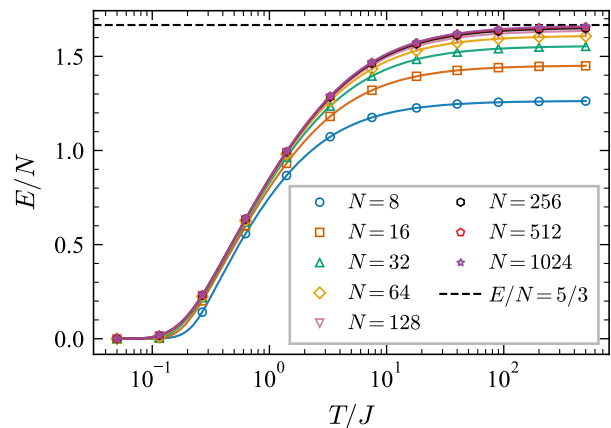


FIG. 3. Energy per queen E/N vs. temperature (logarithmic scale) for $N = 8$ –1024 over the full range $T = 0.05$ – $400 J$. The dashed line marks the analytical $N \rightarrow \infty$ high- T limit $E/N = 5/3$.

TABLE II. C_v/N peak scaling. For $N = 8$ –128, the peak values are from dedicated simulations with dense temperature sampling in $T \in (0.20, 0.30) J$; for $N = 256$ –1024, values are from the standard 280-point grid. The peak height saturates near 1.63 for $N \geq 32$, consistent with the absence of a thermodynamic phase transition.

N	T_{peak}	C_v^{max}/N	error
8	0.281	1.6915	0.0002
16	0.227	1.6783	0.0006
32	0.231	1.6288	0.0005
64	0.237	1.6216	0.0004
100	0.237	1.6229	0.0004
128	0.237	1.6225	0.0004
256	0.2450	1.6238	0.0020
512	0.2400	1.6287	0.0023
1024	0.2325	1.6251	0.0024

dynamic phase transition and identifies the crossover as a Schottky-type anomaly [13]—a broad peak in C_v arising from thermal excitation across a finite energy gap, without any symmetry breaking. Physically, the peak reflects thermal excitation from the non-attacking ground states ($E = 0$) to configurations with a small number of attacking pairs ($E \sim O(1)$); the finite energy gap between these two regimes produces the characteristic broad maximum without critical fluctuations. The peak temperature $T^* \approx 0.235 J$ stabilizes for $N \geq 64$.

The convergence of C_v/N to a definite limiting function has a powerful consequence: since both the high-temperature entropy $S(\infty)/N$ and the ground-state entropy s_0 are independently known, the integral $\int_0^\infty C_v/(NT) dT$ must equal their difference. We exploit this in the next section.

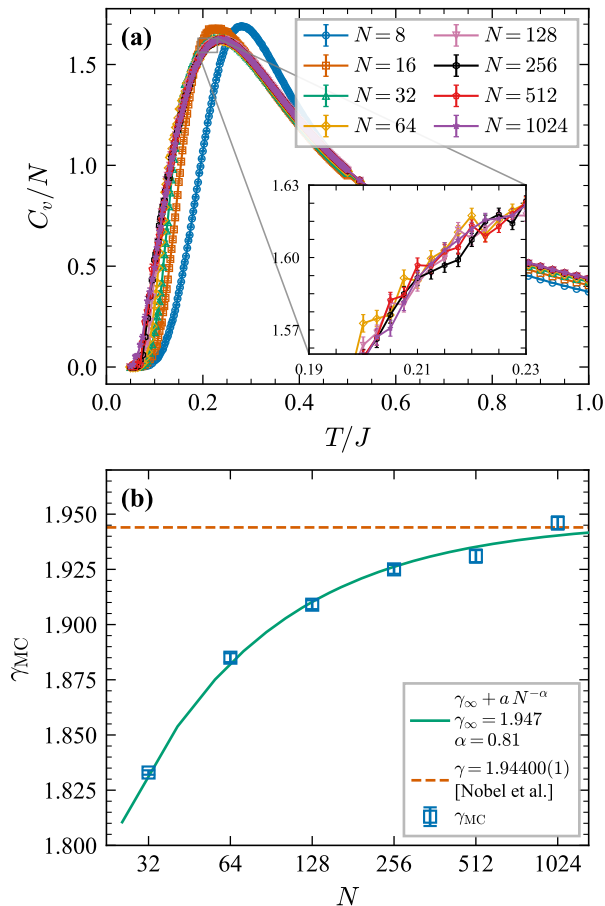


FIG. 4. (a) Specific heat per queen C_v/N vs. T for $N = 8$ – 1024 in the peak region ($T \leq 1 J$, linear scale) with error bars. Inset: zoom into the peak for $N \geq 64$. The curves for $N \geq 32$ collapse onto a single function, confirming convergence to the thermodynamic limit. (b) Extracted Simkin constant $\gamma_{\text{MC}} = \ln N - s_0^{\text{MC}}$ vs. N for $N = 32$ – 1024 . The dashed line marks the precise combinatorial value $\gamma = 1.94400(1)$ [5]. The solid curve is an ad hoc finite-size scaling fit $\gamma_{\text{MC}}(N) = \gamma_\infty + a N^{-\alpha}$, yielding $\gamma_\infty = 1.947 \pm 0.004$ and $\alpha = 0.81 \pm 0.06$. Jackknife-propagated error bars on the data points are plotted but are smaller than or comparable to the symbol size.

V. THERMODYNAMIC INTEGRATION

The convergence of C_v/N to a universal function enables a powerful consistency check. We compute the entropy difference between $T = \infty$ and $T = 0$ in two independent ways and verify that they agree.

Combinatorial route.—At $T \rightarrow \infty$, all configurations are equally probable, so the entropy per queen is

$$\frac{S(\infty)}{N} = \frac{1}{N} \ln \binom{N^2}{N}. \quad (6)$$

For $N \gg 1$, applying the Stirling approximation $\ln n! =$

$$n \ln n - n + \frac{1}{2} \ln(2\pi n) + O(n^{-1}):$$

$$\begin{aligned} \ln \binom{N^2}{N} &= \ln(N^2!) - \ln N! - \ln(N^2 - N)! \\ &= N \ln N - (N^2 - N) \ln(1 - 1/N) + \Delta_S, \end{aligned} \quad (7)$$

where the first two terms come from the $n \ln n - n$ part of Stirling's formula and the correction $\Delta_S = \frac{1}{2} \ln[N^2/(2\pi N(N^2 - N))] = -\frac{1}{2} \ln(2\pi(N - 1))$ collects the subleading logarithms. Expanding $\ln(1 - 1/N) = -1/N - 1/(2N^2) - \dots$, the leading terms give $-(N^2 - N) \ln(1 - 1/N) = N - \frac{1}{2} + O(N^{-1})$, so

$$\frac{S(\infty)}{N} = \ln N + 1 + O\left(\frac{\ln N}{N}\right). \quad (8)$$

At $T = 0$, only ground states contribute: $S(0)/N = \ln Q(N)/N \approx \ln N - \gamma$.

Thermodynamic route.—The fundamental relation

$$S(\infty) - S(0) = \int_0^\infty \frac{C_v}{T} dT \quad (9)$$

relates the entropy difference to the specific heat. Dividing by N and substituting the results above:

$$\int_0^\infty \frac{C_v}{NT} dT = \frac{S(\infty) - S(0)}{N} = 1 + \gamma + O\left(\frac{\ln N}{N}\right). \quad (10)$$

This relation connects a purely thermodynamic quantity—the integrated specific heat on the left—with purely combinatorial constants on the right: the Stirling correction (contributing unity) and the Simkin constant γ .

Rearranging Eq. (10), we can extract the ground-state entropy per queen directly from the Monte Carlo data:

$$s_0^{\text{MC}} = \frac{S(\infty)}{N} - \int_0^\infty \frac{C_v}{NT} dT, \quad (11)$$

where $S(\infty)/N = \frac{1}{N} \ln \binom{N^2}{N}$ is the trivially exact entropy of the uniform distribution over all $\binom{N^2}{N}$ configurations—requiring no knowledge of the ground-state count $Q(N)$ or the Simkin constant. This provides a purely thermodynamic determination of the ground-state degeneracy without direct enumeration; the Simkin–Nobel value $\gamma = 1.94400(1)$ enters only as a benchmark for comparison.

The numerical integration uses 280 temperature grid points spanning from $T = 0.05 J$ to $400 J$; the low- T cutoff contributes negligibly since C_v/T is exponentially suppressed below $T \approx 0.1 J$, and the high- T cutoff at $400 J$ is sufficient because $C_v/T \propto T^{-3}$ decays rapidly, contributing less than 0.01% of the integral beyond this point. The trapezoidal rule on the logarithmic grid introduces discretization errors well below the statistical uncertainty of the Monte Carlo data.

Table III summarizes the results. For $N = 8$ and $N = 16$, where exact values of $Q(N)$ are known ($Q(8) = 92$,

$Q(16) = 14\,772\,512$), s_0^{MC} agrees with the exact $s_0^{\text{exact}} = \ln Q(N)/N$ to within 0.1%, validating the simulation and integration procedure.

For $N \geq 32$, where exact $Q(N)$ is unknown, we use s_0^{MC} to extract the Simkin constant via $\gamma_{\text{MC}} = \ln N - s_0^{\text{MC}}$. The extracted values converge toward the known asymptotic value $\gamma = 1.94400(1)$ [5]: $\gamma_{\text{MC}} = 1.833 \pm 0.001$ ($N = 32$), 1.885 ± 0.002 ($N = 64$), 1.909 ± 0.002 ($N = 128$), 1.925 ± 0.002 ($N = 256$), 1.931 ± 0.003 ($N = 512$), and 1.946 ± 0.003 ($N = 1024$), with the deviation decreasing from 5.7% to 0.11% at $N = 1024$. The dominant source of error at moderate N is the finite-size correction to the Simkin formula, which makes $\gamma_{\text{eff}}(N) = \ln N - s_0(N)$ systematically smaller than the asymptotic γ ; the MC integration itself introduces only sub-percent errors, as confirmed by the $N = 8$ and $N = 16$ benchmarks. The statistical uncertainties on s_0^{MC} and γ_{MC} (Table III) are obtained by propagating jackknife errors on the individual $C_v(T)$ data points through the trapezoidal integration. At $N = 1024$, the propagated uncertainty $\sigma(\gamma_{\text{MC}}) = 0.003$ is small compared to the 0.11% deviation from the asymptotic value, confirming that the dominant source of error is the finite-size correction to the Simkin formula rather than statistical noise.

A finite-size scaling extrapolation (e.g., $\gamma_{\text{MC}}(N) = \gamma_\infty + a N^{-\alpha}$) could in principle improve the infinite- N estimate. Fitting the six data points $N = 32$ – 1024 to this three-parameter form yields $\gamma_\infty = 1.947 \pm 0.004$ with $\alpha \approx 0.81$ [Fig. 4(b), solid curve], consistent with the precise value $\gamma = 1.94400(1)$. However, the functional form of the subleading corrections to $Q(N)$ is not known analytically, making this fitting form ad hoc; the extrapolated value should therefore be regarded as indicative rather than definitive.

The monotonic convergence of γ_{MC} toward $\gamma = 1.94400(1)$ with increasing N —reaching 0.11% accuracy at $N = 1024$ —supports the mutual consistency of the Monte Carlo thermodynamics, the Stirling approximation for $S(\infty)$, and the Simkin combinatorial formula.

VI. TENSOR NETWORK FORMULATION

The geometric constraints of the N -queens problem—specifically, the requirement that no two queens share the same row, column, or diagonal—can be precisely encoded using the matrix product operator (MPO) formalism [16]. Consider, for instance, a single row with 3 sites. Without imposing any constraints, the row admits 2^3 possible configurations, corresponding to $(|0\rangle + |1\rangle)^{\otimes 3}$, where $|0\rangle$ and $|1\rangle$ denote the absence and presence of a queen at each site, respectively. To enforce the condition that each row contains exactly one queen, we construct an MPO as follows:

$$\begin{aligned} & \hat{n}_1 \otimes \hat{n}_0 \otimes \hat{n}_0 + \hat{n}_0 \otimes \hat{n}_1 \otimes \hat{n}_0 + \hat{n}_0 \otimes \hat{n}_0 \otimes \hat{n}_1 \\ & = \mathbf{v}_0 * A * A * A * \mathbf{v}_1^T = M_{\text{row}}, \end{aligned} \quad (12)$$

TABLE III. Ground-state entropy from thermodynamic integration. $s_0^{\text{MC}} = S(\infty)/N - \int_0^\infty (C_v/NT) dT$, where $S(\infty)/N = \frac{1}{N} \ln \binom{N^2}{N}$ is exact. Statistical uncertainties are obtained by propagating jackknife errors on $C_v(T)$ through the trapezoidal integration. For $N \leq 16$, s_0^{MC} is compared with the exact ground-state entropy $s_0^{\text{exact}} = \ln Q(N)/N$. For $N \geq 32$, we extract $\gamma_{\text{MC}} = \ln N - s_0^{\text{MC}}$ and compare with the precise value $\gamma = 1.94400(1)$ [5]. All data use a 280-point temperature grid with 10^8 measurement sweeps per point.

N	s_0^{MC}	s_0^{exact}	γ_{MC}	Deviation
8	0.566 ± 0.000	0.565	—	0.1%
16	1.031 ± 0.001	1.032	—	0.1%
32	1.633 ± 0.001	—	1.833 ± 0.001	5.7%
64	2.274 ± 0.002	—	1.885 ± 0.002	3.0%
128	2.943 ± 0.002	—	1.909 ± 0.002	1.8%
256	3.620 ± 0.002	—	1.925 ± 0.002	1.0%
512	4.308 ± 0.003	—	1.931 ± 0.003	0.69%
1024	4.985 ± 0.003	—	1.946 ± 0.003	0.11%

where the operator $\hat{n}_0 = |0\rangle\langle 0|$ projects onto the empty state (no queen), and $\hat{n}_1 = |1\rangle\langle 1|$ projects onto the occupied state (one queen). The local tensor A of the MPO is

$$A = \begin{pmatrix} \hat{n}_0 & \hat{n}_1 \\ 0 & \hat{n}_0 \end{pmatrix}, \quad (13)$$

and the boundary vectors $\mathbf{v}_0 = (1, 0)$ and $\mathbf{v}_1 = (0, 1)$ indicate that each row starts with zero queens and ends with exactly one queen, respectively. Applying this MPO to the unconstrained state space directly produces a ground state wavefunction that contains all configurations in which each row contains exactly one queen, i.e.,

$$|\Psi\rangle = (\mathbf{v}_0 * A * A * A * \mathbf{v}_1^T)(|0\rangle + |1\rangle)^{\otimes 3}. \quad (14)$$

Similarly, the constraint that there is *at most one* queen along any (anti-)diagonal can also be encoded as an MPO

$$\begin{aligned} & \hat{n}_1 \otimes \hat{n}_0 \otimes \hat{n}_0 + \hat{n}_0 \otimes \hat{n}_1 \otimes \hat{n}_0 + \hat{n}_0 \otimes \hat{n}_0 \otimes \hat{n}_1 \\ & + \hat{n}_0 \otimes \hat{n}_0 \otimes \hat{n}_0 = \mathbf{v}_0 * A * A * A * \mathbf{v}_2^T = M_{\text{diag}}, \end{aligned} \quad (15)$$

The only modification compared to the “exactly one” case is that the boundary vector at the end, previously chosen as $\mathbf{v}_1 = (0, 1)$, should instead be $\mathbf{v}_2 = (1, 1)$. This choice allows for zero or one queen on the constraint line, thus correctly implementing the “at most one” requirement for diagonals and anti-diagonals within the MPO framework.

By combining all MPOs that enforce constraints for rows, columns, and diagonals, we obtain the ground state wavefunction that contains every solution configuration of the N -queens problem. Since each site (i, j) lies at the intersection of four constraint lines, the ground state wavefunction $|\Psi\rangle$ can be written as a tensor network state

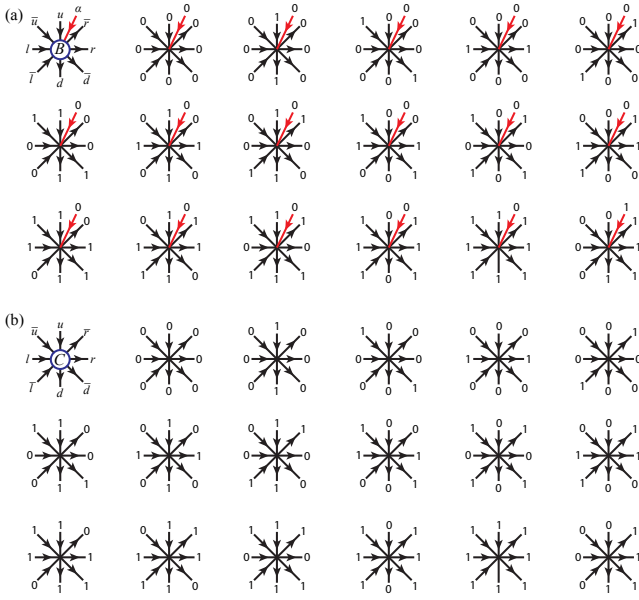


FIG. 5. (a) The 17 nonzero elements of the rank-9 site tensor B [Eq. (16)]. Each diagram shows a lattice site with eight bond indices carrying binary attack signals and one physical index $\alpha \in \{0, 1\}$ (red arrows); the first 16 elements correspond to empty sites ($\alpha = 0$) with all 2^4 combinations of independent pass-through signals along the four constraint channels (column, row, and two diagonal families), and the 17th element (bottom right) represents an occupied site ($\alpha = 1$): all incoming signals are 0 and all outgoing signals are 1. (b) The 17 nonzero elements of the rank-8 site tensor C [Eq. (18)], obtained by summing B over the physical index α . This is the local tensor used in the tensor network contraction for computing $Q(N)$.

with a rank-9 local tensor B at each site, namely,

$$\begin{aligned} B_{ud,lr,\bar{u}\bar{d},\bar{l}\bar{r}}^\alpha &= \sum_{\alpha'\beta'\beta\sigma} A_{ud}^{\alpha\alpha'} A_{lr}^{\alpha'\beta'} A_{\bar{u}\bar{d}}^{\beta'\beta} A_{\bar{l}\bar{r}}^{\beta\sigma} |\sigma\rangle, \\ &= A_{ud}^{\alpha\alpha} A_{lr}^{\alpha\alpha} A_{\bar{u}\bar{d}}^{\alpha\alpha} A_{\bar{l}\bar{r}}^{\alpha\alpha} |\alpha\rangle, \end{aligned} \quad (16)$$

where (u, d) , (l, r) , (\bar{u}, \bar{d}) , (\bar{l}, \bar{r}) are the virtual indices that carry binary signals along the column, row, \searrow -diagonal, and \swarrow -diagonal directions, $\alpha \in \{0, 1\}$ is the physical index labeling the site occupation, and $\alpha', \beta', \beta, \sigma \in \{0, 1\}$ are internal summation indices that collapse to α because A is diagonal in the physical space. Since the local tensor $A_{ij}^{\sigma\sigma}$ of the MPO has only three nonzero elements, namely, $A_{00}^{00} = A_{11}^{00} = 1$ (empty site: signal pass-through) and $A_{01}^{11} = 1$ (occupied site: emit attack signal), the local tensor B of the ground state wavefunction $|\Psi\rangle$ has exactly 17 nonzero elements (see Fig. 5). For an empty site ($\alpha = 0$), each of the four channels independently passes or blocks its signal, giving $2^4 = 16$ elements. For an occupied site ($\alpha = 1$), all incoming signals must vanish and all outgoing signals are emitted, giving one additional element.

Since the ground state wavefunction $|\Psi\rangle$ contains all solution configurations of the N -queens problem, the ex-

act number of solutions $Q(N)$ is obtained by

$$Q(N) = \langle \Psi | (|0\rangle + |1\rangle)^{\otimes N^2}, \quad (17)$$

where $(|0\rangle + |1\rangle)^{\otimes N^2}$ enumerates all possible occupation configurations. Since $(|0\rangle + |1\rangle)^{\otimes N^2}$ is a product state, it is equivalent to contracting each physical index with the vector $(1, 1)^T = |0\rangle + |1\rangle$. As a result, the exact number of solutions $Q(N)$ can be obtained by contracting a tensor network with a bond dimension $D = 2$ local tensor C at each site, namely,

$$C_{ud,lr,\bar{u}\bar{d},\bar{l}\bar{r}} = \sum_{\alpha} B_{ud,lr,\bar{u}\bar{d},\bar{l}\bar{r}}^\alpha, \quad (18)$$

which also has 17 nonzero elements (as shown in Fig. 5 (b)). Figure 6 illustrates the complete tensor network for the 4-queens problem.

More generally, tensor network contraction provides a powerful framework for exact counting in constraint satisfaction problems [14, 18], of which the N -queens problem is a natural instance. The tensor network can be exactly contracted row by row using boundary matrix product state methods [15]. The bond dimension of the boundary MPS grows exponentially with N , so the computational cost is exponential, but the results are free of statistical noise. This makes exact contraction a natural source of benchmarks that complement the Monte Carlo data at moderate N .

Another perspective on the tensor network contraction is the row-by-row transfer matrix \mathcal{T} . Contracting the network row by row with appropriate boundary vectors $|v_0\rangle$ and $\langle v_f|$ gives

$$Q(N) = \langle v_f | \mathcal{T}^N | v_0 \rangle, \quad (19)$$

where $|v_0\rangle = \mathbf{v}_0^{\otimes N} \otimes \mathbf{v}_0^{\otimes(2N-1)} \otimes \mathbf{v}_0^{\otimes(2N-1)}$ is the product of initial boundary vectors for all columns and diagonals (each initialized to $\mathbf{v}_0 = (1, 0)$, signaling no queen seen), and $\langle v_f|$ projects onto the state in which every column carries exactly one queen ($\mathbf{v}_1 = (0, 1)$) while each diagonal carries at most one ($\mathbf{v}_2 = (1, 1)$). A crucial property of \mathcal{T} is that it is *nilpotent*: $\mathcal{T}^{N+1} = 0$. This follows from the column constraint. Each application of \mathcal{T} processes one row and can only increase the number of occupied columns; since there are at most N columns, after $N + 1$ applications all states are annihilated. Consequently, every eigenvalue of \mathcal{T} is exactly zero.

This nilpotent structure stands in sharp contrast to conventional statistical-mechanical models. For the two-dimensional Ising model, for instance, the transfer matrix has a unique largest eigenvalue $\lambda_1 \sim \alpha^N$ for some constant α , and the partition function $Z \sim \lambda_1^N \sim \alpha^{N^2}$ is controlled by this eigenvalue. Standard infinite-size contraction techniques such as CTMRG [17] exploit precisely this spectral dominance. For the N -queens transfer matrix, however, there is no nonzero eigenvalue to target: the solution count $Q(N)$ resides entirely in the matrix elements of \mathcal{T}^N , not in its spectrum. This rules

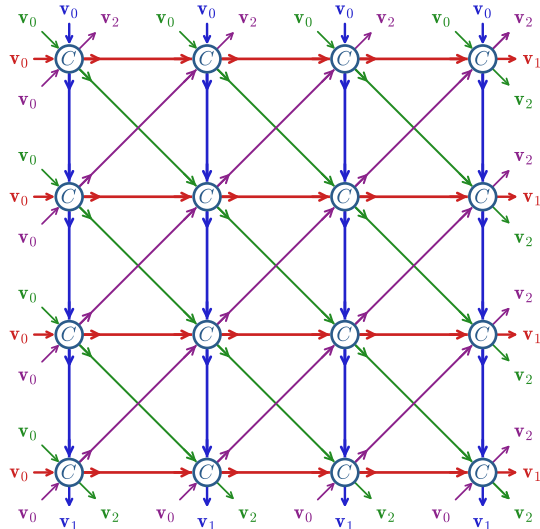


FIG. 6. Tensor network for exact counting of N -queens solutions ($N = 4$). Each node is the rank-8 site tensor C [Eq. (18)]. Arrows on each bond indicate the signal propagation direction: red (row), blue (column), green (\searrow -diagonal), purple (\swarrow -diagonal). Boundary vectors $\mathbf{v}_0 = (1, 0)$, $\mathbf{v}_1 = (0, 1)$, and $\mathbf{v}_2 = (1, 1)$ are labeled at every line terminus, enforcing the queen constraints on each row, column, and diagonal.

out spectral methods (DMRG, VUMPS, CTMRG) and makes finite- N exact contraction the natural framework, as described above.

VII. CONCLUSIONS

We have demonstrated that the Simkin constant γ —a fundamental quantity in combinatorics—can be determined through an independent thermodynamic route. By formulating the N -queens problem as a lattice gas and performing extensive Monte Carlo simulations ($N = 8$ – 1024 , 10^8 sweeps per temperature point), we map out the specific heat C_v/N over the entire temperature range. A key prerequisite is that C_v/N converges to a size-independent function for $N \geq 32$, with a non-divergent

Schottky-type peak at $T^* \approx 0.235 J$ consistent with the absence of a thermodynamic phase transition.

This convergence, combined with the trivially exact high-temperature entropy $S(\infty)/N = \frac{1}{N} \ln \binom{N^2}{N}$, enables a thermodynamic integration of C_v/T that yields the Simkin constant as $\gamma_{\text{MC}} = \ln N - S(\infty)/N + \int_0^\infty (C_v/NT) dT$. The method is validated at $N = 8$ and 16 where exact solution counts are known (agreement within 0.1%), and for larger N produces $\gamma_{\text{MC}} = 1.946 \pm 0.003$ at $N = 1024$, within 0.11% of the precise combinatorial value $\gamma = 1.94400(1)$ [5]. The remaining deviation is dominated by finite-size corrections to the Simkin formula rather than statistical noise, and extending to still larger system sizes would further sharpen the estimate.

These results establish the N -queens lattice gas as an interesting problem from the statistical mechanics perspective. Monte Carlo simulation can be used to estimate the Simkin constant γ . The tensor network formulation presented in Sec. VI provides a complementary exact-enumeration route: it yields $Q(N)$ without statistical noise at moderate N . Together, the two methods cover complementary regimes of N . An open direction is to exploit whether the tools in computational quantum and statistical mechanics will offer new results in this ancient problem in combinatorics.

VIII. DATA AVAILABILITY

The simulation data and analysis code are publicly available on GitHub [19].

IX. ACKNOWLEDGMENTS

The authors acknowledge valuable discussions with Jinguo Liu, Yijia Wang, Qi Yang, Pan Zhang, Youjin Deng and Tao Xiang. This work is supported by the National Natural Science Foundation of China under Grants No. T2225018, No. 12188101, No. T2121001, the Cross-Disciplinary Key Project of Beijing Natural Science Foundation No. Z250005, the Strategic Priority Research Program of the Chinese Academy of Sciences under Grants No. XDB0500000, and the National Key Projects for Research and Development of China Grants No. 2021YFA1400400.

-
- [1] M. Bezzel, Schachfreund, Berliner Schachzeitung **3**, 636 (1848).
 - [2] M. Simkin, The number of n -queens configurations, Adv. Math. **427**, 109127 (2023).
 - [3] C. Bowtell and P. Keevash, The n -queens problem, arXiv:2109.08083 (2021).

- [4] Z. Luria and M. Simkin, A lower bound for the n -queens problem, arXiv:2105.11431 (2021).
- [5] P. Nobel, A. Agrawal, and S. Boyd, Computing tighter bounds on the n -queens constant via Newton's method, Optim. Lett. **17**, 1229–1240 (2023).
- [6] G. Yao and Y. Li, High-performance N -queens solver on GPU: iterative DFS with zero bank conflicts,

- arXiv:2511.12009 (2025).
- [7] D. E. Knuth, *The Art of Computer Programming*, Vol. 4B (Addison-Wesley, 2022), Sec. 7.2.2.
- [8] C. Zhang and J. Ma, Counting solutions for the N -queens and Latin-square problems by efficient Monte Carlo simulations, *Phys. Rev. E* **79**, 016703 (2009).
- [9] N. Polson and V. Sokolov, Counting N queens, arXiv:2407.08830 (2024).
- [10] K. Kawasaki, Diffusion constants near the critical point for time-dependent Ising models. I, *Phys. Rev.* **145**, 224 (1966).
- [11] N. Metropolis, A. W. Rosenbluth, M. N. Rosenbluth, A. H. Teller, and E. Teller, Equation of state calculations by fast computing machines, *J. Chem. Phys.* **21**, 1087 (1953).
- [12] B. Efron, *The Jackknife, the Bootstrap, and Other Resampling Plans* (SIAM, Philadelphia, 1982).
- [13] K. Binder and D. W. Heermann, *Monte Carlo Simulation in Statistical Physics* (Springer, Berlin, 5th ed., 2010).
- [14] N. Kourtis, C. Chamon, E. R. Mucciolo, and A. E. Ruckenstein, Fast counting with tensor networks, *SciPost Phys.* **7**, 060 (2019).
- [15] T. Xiang, *Density Matrix and Tensor Network Renormalization* (Cambridge University Press, Cambridge, 2024).
- [16] F. Fröwis, V. Nebendahl, and W. Dür, Tensor operators: Constructions and applications for long-range interaction systems, *Phys. Rev. A* **81**, 062337 (2010).
- [17] T. Nishino and K. Okunishi, Corner transfer matrix renormalization group method, *J. Phys. Soc. Jpn.* **65**, 891–894 (1996).
- [18] L. Vanderstraeten, B. Vanhecke, and F. Verstraete, Residual entropies for three-dimensional frustrated spin systems with tensor networks, *Phys. Rev. E* **98**, 042145 (2018).
- [19] Z.-Y. Liu, Simulation code and data for the N -queens lattice gas, <https://github.com/LiuZY613/nqueen-lattice-gas>.